



OPEN Resveratrol protects pancreatic beta cell and hippocampal cells from the aggregate-prone capacity of hIAPP

Carlos González-Blanco^{1,2,3,4}, Ángela Cristina Lockwood^{1,2,4}, Beatriz Jiménez^{1,2,4}, Sarai Iglesias-Fortes², Patricia Marqués², Gema García^{1,2,3}, Ana García-Aguilar⁵, Manuel Benito^{1,2,3,4} & Carlos Guillén^{1,2,3,4}✉

Type 2 diabetes mellitus and Alzheimer's disease, are two closely related pathological situations that are connected at the molecular level. In recent years, amylin, which is co-secreted with insulin, has been proposed for being a main actor in this context due to its capacity to form aggregates in a β -sheet-like structure. In a diabetic milieu, there is an increase in the production and secretion of insulin and amylin. We have analysed the role of resveratrol on aggregate formation and in the production of extracellular vesicles with amylin in its interior and in pancreatic β cells overexpressing human amylin (INS1E-hIAPP). Furthermore, we have explored the consequences of the exposition of the conditioned medium derived from INS1E-hIAPP in the hippocampal cell line HT-22 and the role of resveratrol in this cell line. Hippocampal cells were exposed to conditioned media obtained from rat insulinoma 1E overexpressing human amylin in the presence or in the absence of resveratrol. When we exposed HT-22 cells to the conditioned media of INS1E-hIAPP we observed amylin-aggregates inside HT-22 cells. Resveratrol was able to alleviate this effect not only in HT-22 but also in pancreatic β cells. Furthermore, resveratrol decreased the average exosome size produced by the INS1E-hIAPP stimulated with high glucose, diminishing the toxic effect of these exosomes in HT-22 cells. We have uncovered that resveratrol inhibits the aggregation capacity of amylin and it can diminish the deleterious spreading of the toxic protein, to other cell types such as the hippocampal neuron cells, HT-22.

Keywords Amylin, Beta cell, Beta-sheet-like aggregates, HT-22, Mitochondrial dynamics, Resveratrol

Abbreviations

ATP	Adenosine triphosphate
BIP	Binding protein
DMSO	Dimethyl sulfoxide
Drp1	Dynamin-related protein 1
ER	Endoplasmic reticulum
FBS	Foetal bovine serum
hIAPP	Human islet amyloid polypeptide or amylin
MEF	Mouse embryo fibroblast
MFN1	Mitofusin 1
MFN2	Mitofusin 2
mTOR	Mechanistic target of rapamycin
mTORC1	Mechanistic target of rapamycin complex 1

¹CIBER of Diabetes and Related Metabolic Disorders, Instituto de Salud Carlos III, 28040 Madrid, Spain. ²Department of Biochemistry and Molecular Biology, Faculty of Pharmacy, Complutense University of Madrid, Plaza Ramón y Cajal s/n, Ciudad Universitaria, 28040 Madrid, Spain. ³Department of Biochemistry and Molecular Biology, Faculty of Pharmacy, Complutense University of Madrid, IdISSC, Madrid, Spain. ⁴P2022/BMD-7227, MOIR-ACTOME-CM, Dirección General de Investigación e Innovación Tecnológica (DGIIIT), Consejería de Educación y Universidades, Comunidad de Madrid, Madrid, Spain. ⁵Department of Pharmacology, Pharmacognosy and Botany, Faculty of Pharmacy, Complutense University of Madrid, Madrid, Spain. ✉email: cguillen@ucm.es

mTORC2	Mechanistic target of rapamycin complex 2
NaF	Sodium fluoride
OPA1	Optic atrophy 1
L-OPA1	Large isoform optic atrophy 1
S-OPA1	Short isoform optic atrophy 1
PBS	Phosphate buffered saline
PMSF	Phenylmethylsulfonyl fluoride
T2DM	Type 2 diabetes mellitus
TSC2	Tuberous sclerosis complex 2
TTBS	Tween-Tris-buffered saline
ULK1	Unc-51 like autophagy activating kinase 1

Type 2 diabetes mellitus (T2DM) is a progressive and multifactorial disease which is characterised by insulin resistance and the appearance of hyperinsulinemia during the first stages of the disease. As a consequence, pancreatic β cells are overwhelmed by its increased capacity to produce and secrete more insulin, which is known as the pre-diabetic stage¹. Under this compensatory situation that occurs in β cells during the progression to T2DM, mTORC1 signalling pathway is one of the key regulators of pancreatic cell mass². There are several factors involved in pancreatic β cell failure and apoptosis with the appearance of a frank diabetes situation, including oxidative stress, endoplasmic reticulum (ER) stress, mitochondrial dysfunction, and an alteration in autophagy³. Oxidative stress is a very important event in these cells since pancreatic β cells are extremely sensitive to this damage because of a very poor antioxidant capacity⁴. Apart from the factors previously mentioned that affect pancreatic β cell viability, dedifferentiation is another mechanism that could be involved in the appearance of a diabetic phenotype⁵.

Amylin is a protein that is co-stored in the same secretory granules, and it is co-secreted with insulin. Amylin has a great variety of functions in the brain and in the periphery including the regulation of food intake and the delay of gastric emptying among others⁶. Very importantly, depending on amylin's primary structure, the protein presents different aggregation capacity^{7,8}. There are different forms of amylin including, the soluble, which is monomeric and non-toxic form, and the aggregated forms. But there are different aggregates intermediates, including oligomers, protofibrils and fibrils, being the pathologic forms the oligomeric ones. In the other hand, the fibrillar structures are considered non-pathogenic^{7,8}. The overproduction of human amylin (hIAPP) in pancreatic β cells lead to different alterations including an increase in oxidative stress, with the appearance of a boosted nitro tyrosine level associated with the appearance of polyubiquitinated aggregates, mitochondrial dysfunction and an impaired mitophagy. In addition to all the changes indicated, a hyperactivation of mTORC1 signalling pathway has been also observed. This induction in mTORC1 is probably due to an increase in the degradation of the negative regulator of mTORC1 activation, which is the tuberous sclerosis complex 2 (TSC2)⁹. mTOR is a protein that can be taken part into two different complexes; mTORC1 and mTORC2. Both complexes are involved in the control of metabolic functions and its dysfunction facilitates the appearance of different diseases such as T2DM, obesity and neurodegeneration¹⁰. Very importantly, mTOR is also related with endoplasmic reticulum (ER) stress (ER-stress) which, if it is chronically activated, could be involved in the apoptosis of the cells^{2,11}. ER-stress is an adaptive mechanism which is involved in the sensing of a correct loading and folding of proteins in the ER. When there is an increased production of proteins and the ER is overwhelmed, several sensors (PERK, IRE1- α and ATF6), located in the ER membrane activates for avoiding a chronic ER-stress, which is deleterious for the cells. These three sensors are coupled, under normal conditions, with a luminal resident chaperone known as Bip. When there is an accumulation of protein synthesis demand, Bip dissociates from the sensors and become activated¹².

It is known that T2DM is clearly associated with different neurodegenerative processes such as Alzheimer's and Parkinson's disease. This strong correlation between these two pathologies, is described as type 3 diabetes, and is related with the appearance of brain insulin resistance^{13,14}. Very recently, it has been proposed that amylin and its amyloidogenic capacity could be a key regulator connecting T2DM and neurodegeneration¹⁵⁻¹⁸. Importantly, for reducing these toxic oligomers in T2DM, neurodegenerative diseases, including Alzheimer's disease, Parkinson's disease and others, several strategies have been proposed. Despite the fact that the mechanism of toxicity could vary by the distinct oligomers in the different diseases, all of them share structural features that can be used for a common therapeutic strategy. One of these strategies is using small compounds, including resveratrol^{19,20}. This protective effect has been determined using in vitro approaches in either the neural crest-derived cell line N2a and human embryo kidney cells (HEK) stably transfected with mutant forms found in Alzheimer's disease patients²¹. Moreover, the protection of resveratrol has been proven using animal models of Alzheimer's disease, including an improvement in memory loss and cognitive decline, a decrease in oxidative stress and a reduction of amyloid deposits²².

In the last years, mitochondrial dynamics have arisen as a potential target of regulation controlling energetic status of the cell, which is known to be drastically altered in pathological situations such as T2DM and Alzheimer's disease²³. Mitochondria are not static organelles and can modify their interaction with other surrounding mitochondria by fusion or can be divided into smaller units, which is called fission, depending on the energetic requirements of the cell^{24,25}. Mitochondrial fusion permits an enhancement in the production of ATP and mitochondrial fission is associated on many occasions with mitochondrial degradation^{24,25}.

We have uncovered that conditioned media obtained from pancreatic β cells with an overexpression of hIAPP and exposed to mouse hippocampal cells, generated similar changes to that which we observed in pancreatic β cells with the overproduction of hIAPP, including an induction of ER-stress, mTORC1 hyperactivity and an impaired autophagy²⁶. There are different strategies for treating metabolic and neurodegenerative diseases but they all present different side effects that could have detrimental consequences in patients. Then, natural products

and, more specifically polyphenols such as resveratrol, possess multiple beneficial effects, protecting against the oxidative stress, alleviating ER stress, and facilitating autophagy, being promising treatments to combat all these diseases²⁷.

Here, we report the effect of resveratrol in the modulation of mitochondrial dysfunction and hIAPP production through the modulation of mTORC1 and ER-stress signalling pathways and, how these alterations can modify hippocampal cells' fate connecting T2DM and neurodegeneration through amylin-induced oxidative stress.

Materials and methods

Cell lines

Rat insulinoma cell line INS1E were kindly provided by P. Maechler (Université de Genève, Geneva, Switzerland); INS1E overexpressing human amylin (INS1E-hIAPP) were generously supplied by Anna Novials (IDIBAPS, Barcelona, Spain). INS1E cell lines were cultured in 10% FBS RPMI 1640 medium supplemented with 1 mM sodium pyruvate, 10 mM HEPES and 50 μ M 2-mercaptoethanol. Mouse hippocampal cell line HT-22 was donated by Rafael Simó (Vall D'Hebron Research Institute, Barcelona, Spain) and cultured in 10% FBS DMEM High Glucose medium supplemented with 20 mM HEPES. The cell lines were maintained at 30,000 cells/cm² changing the medium every 2 days. For performing the experiments with the conditioned media (CM), we previously seeded the INS1E-hIAPP and obtained the 48 h-CM. The day before the obtention of the CM from INS1E-hIAPP, we seeded HT-22 cells at 20,000 cells/cm². Then, after collecting the CM, we changed the medium of HT-22 cells and we added the new medium for the corresponding period of time.

Antibodies and reagents

Anti-TSC2 (#4308S), anti-p70S6K (#9202S), anti-phospho p70S6K (#9205S), anti-ULK1 (#8054S), anti-phospho ULK1 (#14202S), anti-PERK (#3192S), anti-phospho PERK (#3179S), anti-BIP (#3177S), anti-eIF2 α (#9722S), anti-phospho eIF2 α (Ser 51) (#9721S), anti-Drp1 (#8570S) and anti-phospho Drp1 (S616) (#3455S) were obtained from Cell Signalling Technology (Beverly, MA). Anti-mfn1 (ab104274) and anti-mfn2 (ab56889) were obtained from Abcam (Cambridge, UK). Anti-OPA1 (#612606) was obtained from BD Biosciences (San Jose, CA). Anti-amylin (NBP1-07579) for western blot analysis was obtained from Novus Biologicals. Secondary antibodies HRP-conjugated used: anti-Rabbit (NA934) and anti-Mouse (NA931) were obtained from GE Lifesciences. All the antibodies were prepared at 1:1000 dilution in TTBS + 5% BSA. For IF secondary antibody Donkey anti-Rabbit IgG (#A-21207) Alexa Fluor 594 obtained from Invitrogen was used and the dilution of these antibodies were 1:100 prepared in the blocking buffer (3% BSA + 0.1% Tween 20 in PBS (PBT)). The primary antibodies for the immunofluorescence were prepared in the blocking buffer at 1:50 dilution. Resveratrol (R5010) and dynasore (D7693) were obtained from Sigma-Aldrich (St. Louis, MO). Exo-FBS™ (EXO-FBS-250 A-1) and Exo-Quick reagent. TC™ (EXOTC50A-1) were obtained from SBI Bionova®. Poly-L-ornithine hydrobromide (P3655) was obtained from Sigma-Aldrich. In collaboration with the organic chemistry department of our faculty, we have used an organic fluorescent compound (known as MG5), which is capable to detect β -sheet aggregates, as it was originally described²⁷.

Treatments and conditioned culture media

INS1E-hIAPP cells were grown on the plate to 80% confluency. At that point their medium was changed to INS1E-hIAPP cells RPMI medium enriched in glucose (17 mM). After 24 h, the medium (conditioned medium) was collected and added to the HT-22 cells for 24 h. Resveratrol was diluted in pure ethanol and administered to cells at a final concentration of 30 μ M. Dynasore was diluted in DMSO at a final concentration of 80 μ M. In the experiment with the INS1E and HT-22 cell lines, resveratrol was administered during the last 4 h of the corresponding experiment. In the experiment with HT-22 cell lines, dynasore pre-treatment was administered 90 min before the addition of CM. A refill of dynasore was added after the CM administration.

Exosome purification

To carry out the isolation and purification of exosomes from medium of cell culture, INS1E-hIAPP cells were grown until reaching a confluence of the 70–80%, and subsequently, were maintained in complete RPMI 1640 culture medium supplemented with exosome-depleted serum Exo-FBS™ (SBI Bionova®) enriched in glucose (17 mM) for 24 h. After this time, media were collected and centrifuged at 3000 \times g for 15 min to discard cell debris. Subsequently, these media were filtered using a 0.22 μ m filter pore size to rule out extracellular vesicles larger than that size in the solution. Media were then mixed with the Exo-Quick reagent. TC™ (SBI Bionova®) in a ratio of 5 mL of medium for every 1 mL of reagent, and incubated gentle shaking overnight at 4 °C. Next day, the mixture was centrifuged at 1500 \times g for 30 min, obtaining a precipitate corresponding to the isolated exosomes. Exosomes were resuspended in 1X PBS and were stored at 4 degrees until use.

Western blotting

After the different treatments, cells were washed twice with PBS 1 \times and lysed with a lysis buffer [Nonidet-P40 1% (v/v), Tris-HCl 50 mM, EDTA 5 mM, EGTA 5 mM, NaCl 150 mM, NaF 20 mM, pH 7.5, PMSF 1 mM, aprotinin 10 μ g/ml, leupeptin 2 μ g/ml and sodium orthovanadate 1 mM). The cell lysate was allowed to stand for 10 min on ice. Subsequently, each sample was sonicated and centrifuged at 13,000 rpm for 15 min, collecting the supernatant fraction. Protein concentration determination was achieved by the Bradford dye method, using de Bio-Rad® (Hercules, CA) reagent and BSA as standard. Equal amounts of protein (10 μ g) were submitted to electrophoresis and after SDS-PAGE gels were transferred to Immobilon P PVDF membranes (Merck Millipore, Burlington, MA) following the Western Blot wet transfer protocol. Then, membranes were blocked with TTBS [Tris-HCl 10 mM, NaCl 150 mM, pH 7.5 and Tween-20 0.05% (v/v)] + BSA 5% 1-hour gentle shaking and incubated overnight with primary antibodies at 4 °C at 1:1000 dilution in TTBS + 5% BSA. The

next day, the membranes were washed 3 times for 10 min with TTBS and incubated at room temperature with the corresponding secondary antibody diluted in TTBS at 1:1000 dilution. After 1 h, the secondary antibody was removed from the membranes and three 10-min washes were performed with TTBS. The corresponding bands were visualised using the ECL Western blotting protocol (GE Healthcare, Little Chalfont, UK).

Immunofluorescence

Cells were grown on glass coverslips and fixed using paraformaldehyde 4% solution during 20 min, permeabilized in PBS with 0.5% Triton X-100 for 15 min, and then blocked with blockage solution (3% BSA, 0.1% Tween 20 in PBS) for 1 h. Cells were incubated overnight at 4 °C with primary antibody (1:50 in blocking solution). After the incubation, coverslips were incubated with the corresponding secondary antibody at a dilution of 1:100 for 1 h 30 min. For MG5 imaging, the organic compound was diluted in DMSO to 10 µM, and cells were incubated with the solution for 20 min before DAPI staining. For exosome immunofluorescence, coverslips were pre-treated with Poly-L-Ornithine 20 µg/ml for 2 h at 37 °C, rinsed twice with sterile water, to provide surface charge. Purified exosomes were deposited on the surface of the coverslip overnight so that they would stick to the surface. The following day they were fixed using paraformaldehyde 4% and the same protocol as the cells was carried out. All the images were captured by Laser Scanning Confocal Microscopy using an Olympus FV1200 with the software Olympus FLUOVIEW Ver 4.2. For immunofluorescence quantification of both amylin (red channel) and MG5 (green channel), we have used the mean fluorescence intensity of several images. We quantified at least 300 cells of 2–3 different experiments. The threshold was obtained automatically using the Costé's automatic threshold. For the immunofluorescence analysis, multiple planes were examined for each data point. In each plane, the fluorescence intensity was recorded and divided by the number of cells located in that plane, yielding the fluorescence intensity per cell for that specific plane. This process was repeated until at least 300 cells were counted at each data point.

Dynamic light scattering (DLS)

The size of the extracted exosomes was measured using a Zetasizer Nano ZS system (Malvern Instruments, Malvern, U.K.). For DLS measurements, 10 µL exosome aliquots were diluted in 990 µL of PBS (1:100) and then gently mixed to provide a homogeneous solution, and then 1 mL was transferred to a disposable cuvette for size measurements. Several independent aliquots were analysed and five measurements were taken for each aliquot. The data were acquired and analysed using Dispersion Technology Software (DTS) (V7.01) supplied by the Malvern Zetasizer Nano-ZS.

Statistical analysis

Statistically significant differences between mean values were determined using either the unpaired Student's *t*-test or ANOVA test using as post hoc the Tukey's multiple comparison test. All the statistical analysis was performed with the Graphpad statistical analysis software package. Differences were considered statistically significant at $p < 0.05$ (* $p < 0.05$; ** $p < 0.01$; *** $p < 0.005$, **** $p < 0.0005$).

Results

Resveratrol increases the appearance of soluble amylin in pancreatic β cells

In order to analyse the soluble amylin protein, we will use an antibody which detects amylin of human, mouse and rat origin in a soluble or monomeric state. It is important to indicate that this antibody does not react against the aggregate forms of amylin. First of all, we observed an increase in the basal levels of amylin in INS1E-hIAPP cells compared with INS1E-WT cells. In INS1E-WT cells there was an increase in soluble amylin using either western blot analysis or immunofluorescence under basal glucose or high glucose with or without resveratrol (Fig. 1). When we analysed INS1E-hIAPP cells by western blot, there was a significant reduction in amylin protein levels in response to resveratrol (Fig. 1A). However, under high glucose conditions the protective role of resveratrol in reducing amylin in these cells was impaired, and we could detect a similar amount of soluble amylin under both situations, under basal or high glucose conditions, in the absence or in the presence of resveratrol (Fig. 1A). When we analysed INS1E-hIAPP by immunofluorescence, there was a significant increase in amylin in response to resveratrol. Very importantly, after exposition to high glucose, there was a dramatic reduction in amylin that was partially recovered when we added resveratrol (Fig. 1B).

Resveratrol protects INS1E-hIAPP cells from an altered energetic homeostasis through changes in mitochondrial dynamics, mTORC1 and ER-stress signalling pathways

In order to analyse the consequences of an altered mitochondrial dynamics in the energetic homeostasis into more detail, we decided to measure several important proteins involved in either mitochondrial fusion (Mfn2 and OPA1) and mitochondrial fission (Drp1 and its phosphorylated form)²⁵. Comparing INS1E-WT with INS1E-hIAPP we observed that, at basal state, INS1E overexpressing hIAPP presented a statistically significant increase in Mfn2 protein levels. Mfn1 protein showed a tendency to increase with a concomitant reduction in the phosphorylation status of Drp1 (Fig. 2A). These data indicates that mitochondria from INS1E-hIAPP tend to be preferentially in a pro-fusion state. OPA1 is a protein that can be found in two different isoforms; a longer version, which is involved in fusion and a shorter version, involved in fission^{24,25}. However, we observed a reduction in the L-OPA-1/S-OPA1 ratio in these cells, suggesting that, accordingly to this parameter, there is an increased in the fission state. All these data indicates that mitochondrial network is under a balanced situation between fusion and fission parameters. Importantly, under high glucose conditions, there was an expected decrease in fusion, by a reduction in the L-OPA1/S-OPA1 ratio in INS1E-WT cells with no modifications in any of the other parameters of either fusion (Mfn1 and Mfn2) or fission (phospho-Drp1). These data suggest that, under high glucose, there is a switch towards a mitochondrial fission scenario. Paradoxically, in INS1E-

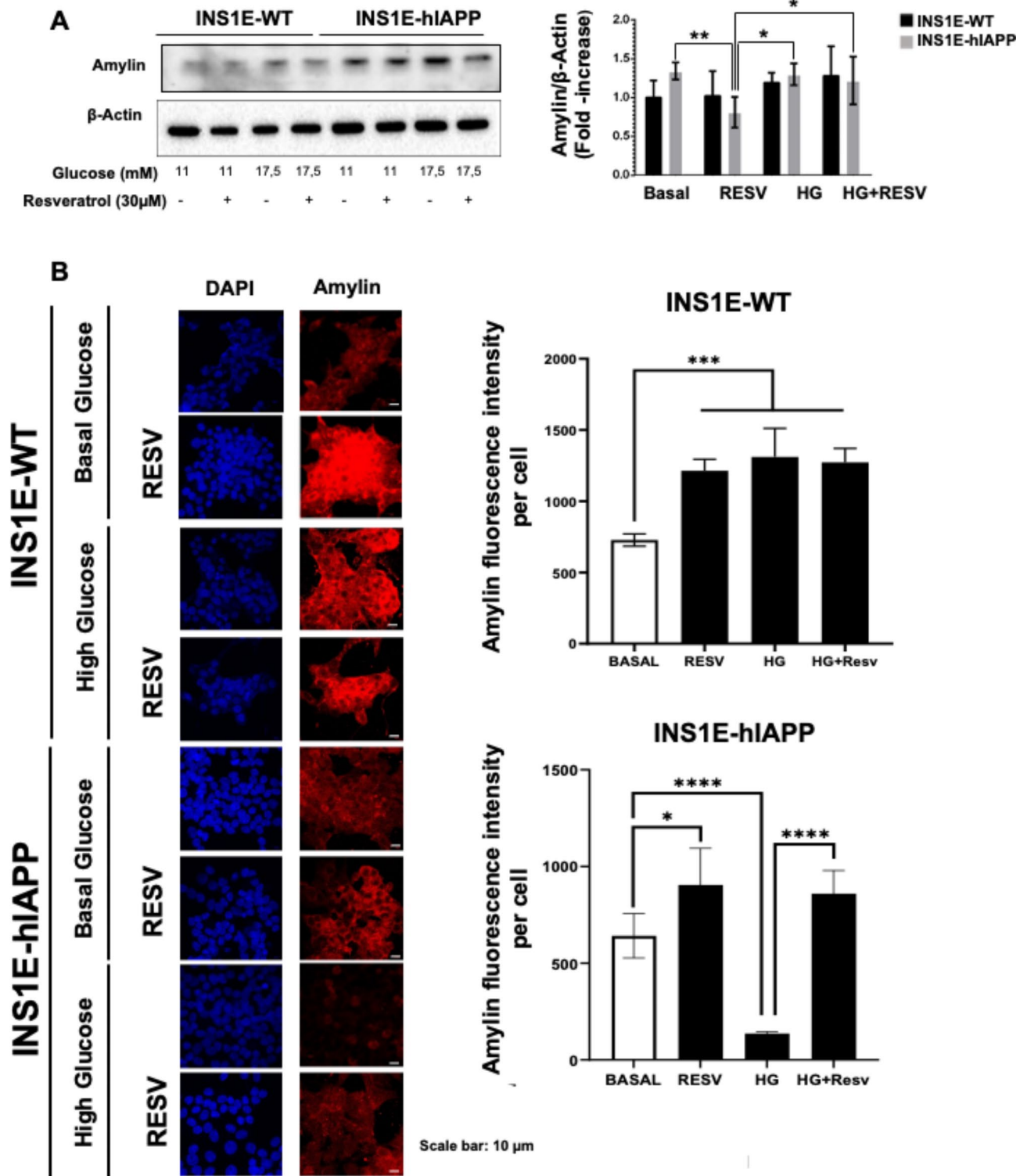


Fig. 1. Resveratrol increases the appearance of soluble amylin in pancreatic β cells. **(A)** Immunoblot analysis of amylin, using β actin as loading control, in the cell extracts of both INS1E-WT and INS1E-hIAPP pancreatic β cell lines exposed to either low or high glucose levels with and without Resveratrol 30 μ M 4 h ($n=5$). The plot indicates the quantification data of Amylin/ β -actin ratio under the different conditions. Data represent the mean \pm standard error of the mean (SEM) ($n=5$). * $p < 0.05$; ** $p < 0.01$ by unpaired Student's t -test. **(B)** Immunofluorescence staining using an antibody against amylin in the different pancreatic β cells under either low or high glucose levels with and without Resveratrol 30 μ M 4 h. DAPI staining was used to detect nuclei. The plot indicates the quantification data of Amylin fluorescence intensity under the different conditions. *** $p < 0.005$; **** $p < 0.0005$ by unpaired Student's t -test.

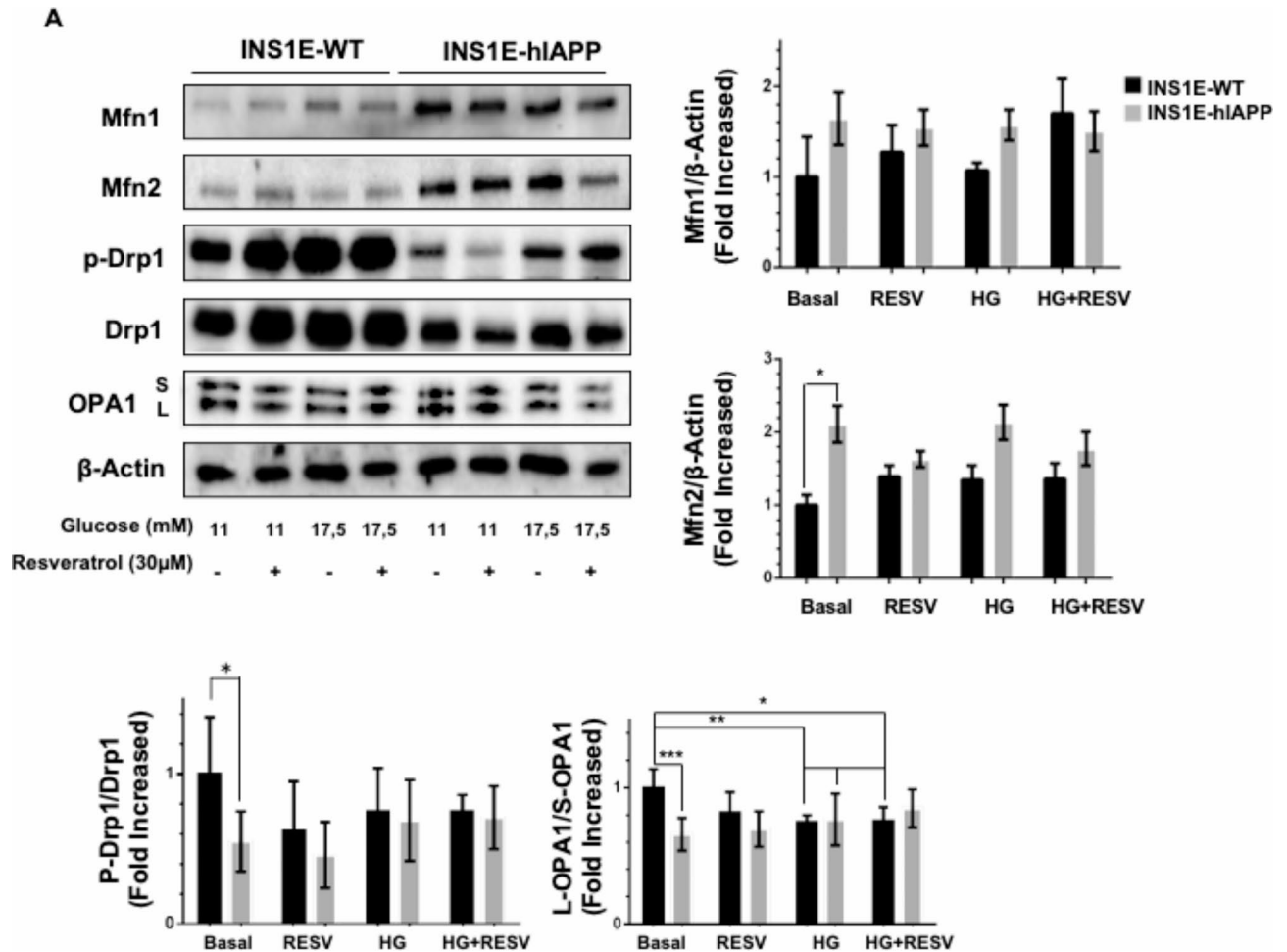


Fig. 2. Resveratrol protects INS1E-hIAPP cells from an altered energetic homeostasis through changes in mitochondrial dynamics, mTORC1 and ER-stress signalling. **(A)** Immunoblot analysis of Mfn1, Mfn2, p-Drp1, Drp1, OPA1, HADHA, using β actin as loading control, in the cell extracts of both INS1E-WT and INS1E-hIAPP pancreatic β cell lines exposed to either low or high glucose levels with and without Resveratrol 30 μ M 4 h ($n = 5$). The plot indicates the quantification data of Mfn1, Mfn2, p-Drp1/Drp1, L-OPA1/S-OPA1 HADHA/ β -actin ratio under the different conditions. Data represent the mean \pm standard error of the mean (SEM). * $p < 0.05$; ** $p < 0.01$ using ANOVA test using as post hoc the Tukey's multiple comparison test. **(B)** Immunoblot analysis of p-p70, p70, p-ULK1 757, ULK1 using β actin as loading control, in the cell extracts of both INS1E-WT and INS1E-hIAPP pancreatic β cell lines exposed to either low or high glucose levels with and without Resveratrol 30 μ M 4 h ($n = 5$). The plot indicates the quantification data of Mfn1, Mfn2, p-p70/p70, p-ULK1 757/ULK1 ratio under the different conditions. Data represent the mean \pm standard error of the mean (SEM). * $p < 0.05$ by unpaired Student's t -test **(C)** Immunoblot analysis of BIP, p-eIF2 α , eIF2 α , p-PERK, PERK, using β actin as loading control, in the cell extracts of both INS1E-WT and INS1E-hIAPP pancreatic β cell lines exposed to either low or high glucose levels with and without Resveratrol 30 μ M 4 h ($n = 5$). The plot indicates the quantification data of BIP, p-eIF2 α /eIF2 α , p-PERK/PERK ratio under the different conditions. Data represent the mean \pm standard error of the mean (SEM). * $p < 0.05$; ** $p < 0.01$ by unpaired Student's t -test.

hiAPP under a high glucose situation the switch in mitochondrial dynamics observed in INS1E-WT did not occur, with a maintenance of high Mfn1 and Mfn2 protein levels compared with INS1E-WT cells (Fig. 2A). Previous results indicated that in INS1E-hIAPP cells there was a basal induction of mTORC1 signalling pathway and an increased susceptibility to ER-stress⁹. Then, we explored the possibility that resveratrol could exert its action through the modulation of mTORC1 and ER-stress signalling pathways. Firstly, we corroborated the basal hyperactivation of the mTORC1 signalling pathway in INS1E-hIAPP compared with INS1E-WT cells (Fig. 2B). There was an activation of mTORC1 signalling in response to all of the treatments in INS1E-WT cells. However, in INS1E-hIAPP, the hyperphosphorylation state of ULK1 was significantly reduced in response to resveratrol (Fig. 2B). When we performed the analysis of ER-stress we did not find any relevant change in INS1E-WT cells. Interestingly, when we treated INS1E-hIAPP with resveratrol, there was an increase in the ER-stress. Very importantly, when INS1E-hIAPP cells were stimulated with high glucose, although there was

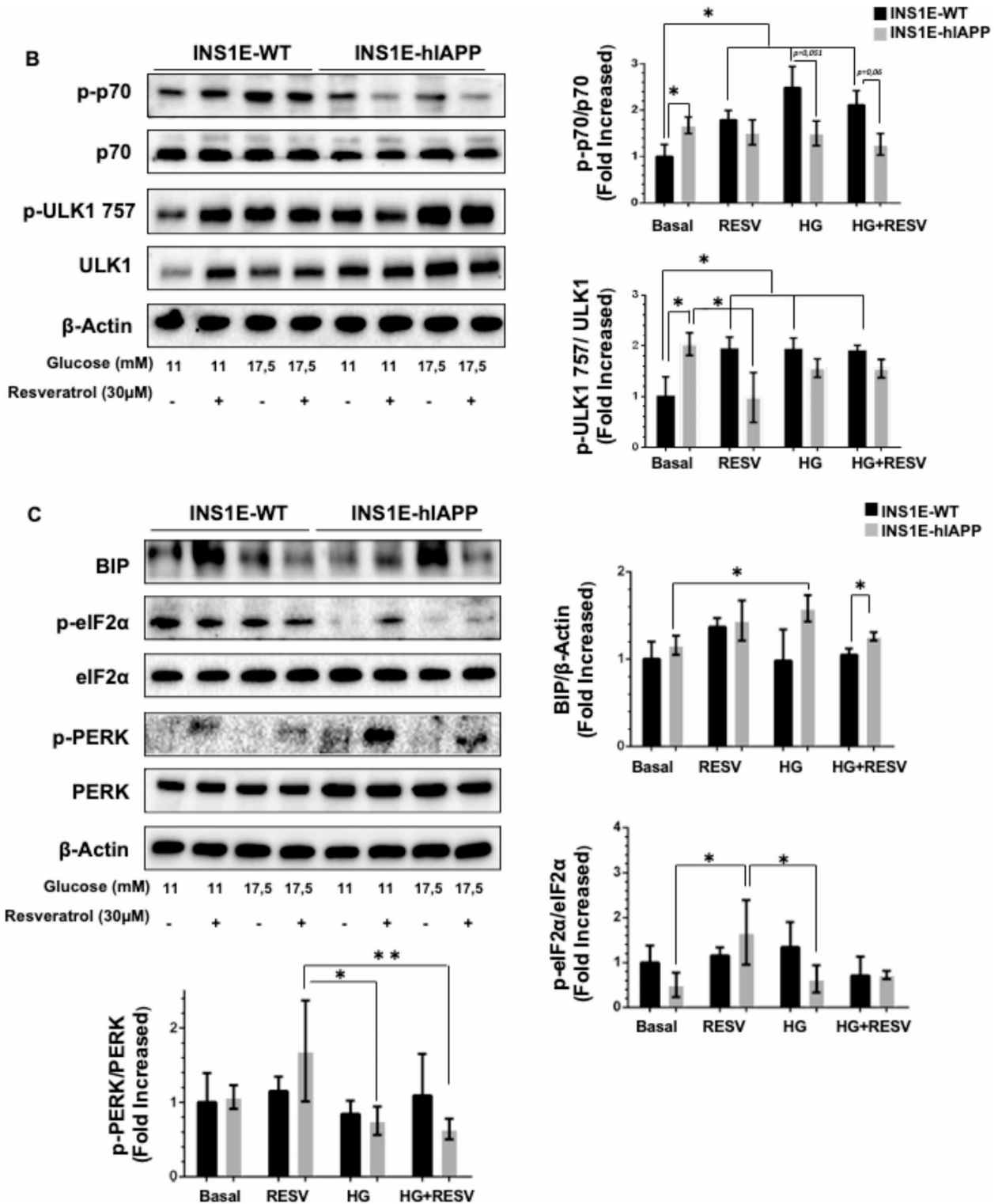


Figure 2. (continued)

a maintained signal of BIP, there was a significant reduction in the activation of the unfolded protein response (UPR) signalling pathway, of both phospho-eIF2α/ eIF2α and phospho-PERK/PERK ratios (Fig. 2C).

Conditioned medium from INS1E-hIAPP permits an accumulation of aggregates in the hippocampal cells HT-22 in an endocytosis-dependent manner

To understand the link between pancreatic β cells and the hippocampus, we exposed HT-22 to the conditioned media (CM) obtained from INS1E-hIAPP at different times. We observed a progressive accumulation of

aggregates, stained by the MG5 compound (that detects aggregates when forming a β -sheet structure) in HT-22 cells²⁸, being statistically significant at 24 h (Fig. 3A). This accumulation of aggregates in HT-22 cells in response to the CM derived from INS1E-hIAPP was also corroborated using Thioflavin T staining (Supplementary Fig. 1) and not when the CM derived from INS1E-WT cells (Supplementary Fig. 2). When we pre-treated the cells with

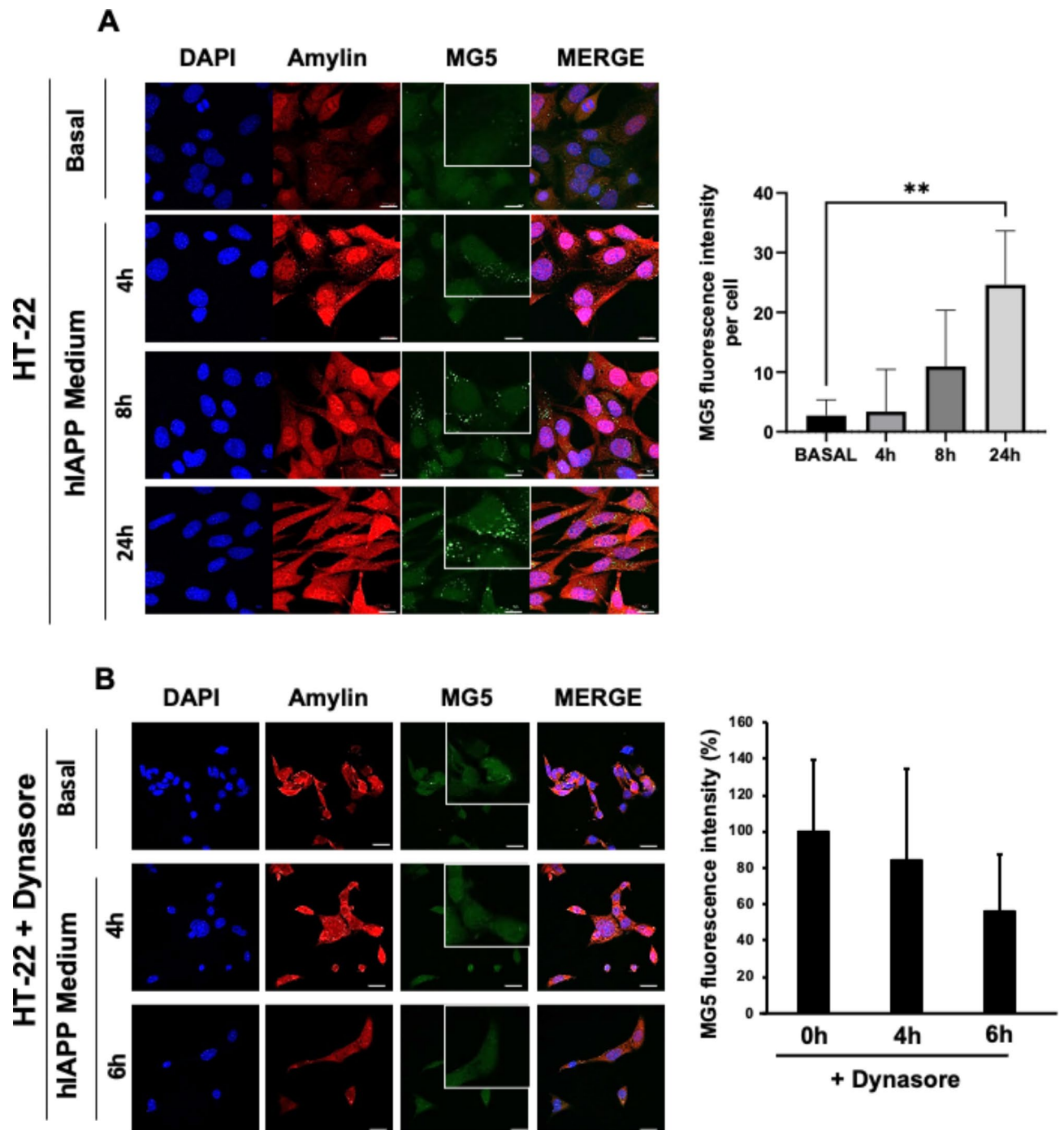


Fig. 3. Conditioned medium from INS1E-hIAPP permits an accumulation of aggregates in the hippocampal HT22 cells in an endocytosis-dependent manner. **(A)** Immunofluorescence staining using an antibody against amylin and MG5 compound, which detects amylin aggregates in the HT-22 cells exposed to conditioned media for 0, 4, 8 and 24 h. DAPI staining was used to detect nuclei. The plot indicates the quantification data of MG5 fluorescence intensity under the different conditions. **** $p < 0.0005$ using unpaired Student's *t*-test. **(B)** Immunofluorescence staining using an antibody against amylin and MG5 compound in the HT-22 cells exposed to conditioned media for 0, 4 and 6 h with dynasore at 80 μ M for 90 min before adding the conditioned medium. DAPI staining was used to detect nuclei. The plot indicates the quantification data of MG5 fluorescence intensity under the different conditions.

dynasore, a blocker of the GTPase activity of dynamins, which are essential in the control of the endocytosis and hence, of the endocytic particle formation²⁹, we did not detect the presence of aggregates inside HT-22 cells, indicating that endocytosis is an essential step for inducing the aggregation capacity of CM obtained from INS1E-hIAPP in HT-22 (Fig. 3B).

Resveratrol impairs the production of amylin-bearing extracellular vesicles in INS1E-hIAPP pancreatic β cells

Previously, we established that CM from INS1E-hIAPP cells promotes aggregate formation in HT-22 cells, a process impeded by hindering endocytic processes. Furthermore, we confirmed that these cells produce extracellular vesicles (EVs) containing amylin²⁶. Subsequently, we investigated whether resveratrol could influence the production of these amylin-bearing EVs. Upon purification, it became evident that, under high glucose conditions, there was an increase in the size of EVs isolated from INS1E-hIAPP (Fig. 4A). The presence of amylin within these EVs was confirmed through immunofluorescence, exclusively in the case of INS1E-hIAPP cells (Fig. 4B).

Significantly, resveratrol treatment resulted in a reduction in the number of particles with the highest size and a simultaneous emergence of smaller structures (Fig. 4A). This observation suggests that resveratrol has a discernible effect on the capacity of cells to produce amylin-bearing EVs, particularly under conditions of high glucose.

Hippocampal HT-22 cells are protected with resveratrol from the aggregate-prone capacity of hIAPP

Taking the analysis in a step further, we explored whether resveratrol could exert a protective role against the aggregation capacity of CM, similar to what was observed in INS1E-hIAPP. This investigation was conducted over two distinct time periods in HT-22 cells. Under basal conditions, we detected the presence of amylin inside the cells, signifying their ability to produce the protein. While there was a time-dependent increase in amylin levels, exposure to CM from INS1E-hIAPP for 24 h resulted in a notable rise in amylin protein levels. This increase was somewhat mitigated, albeit not reaching statistical significance, following the addition of resveratrol during the last 4 h of the experiment (Fig. 5A).

To corroborate these findings, we conducted an immunofluorescence analysis at the 24-hour mark, using both amylin and aggregates with the MG5 compound, in the presence or absence of resveratrol. We chose this time point based on our previous observations (Fig. 3A), determining it to be the optimal period for aggregate

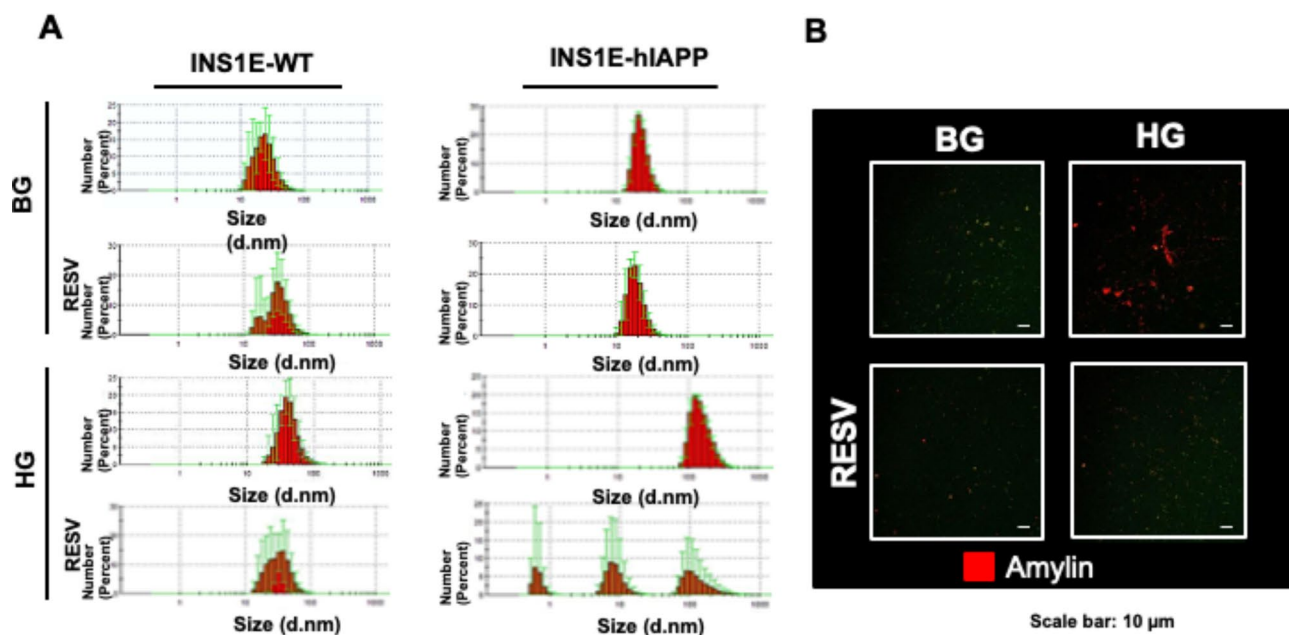


Fig. 4. Resveratrol impairs the production of amylin-bearing extracellular vesicles in INS1E-hIAPP pancreatic β cells. (A) Dynamic light scattering analysis of the exosomes purified from the different pancreatic β cells ($n = 3$). (B) Immunofluorescence staining using an antibody against amylin of the exosomes purified from INS1E-hIAPP exposed to either low or high glucose levels.

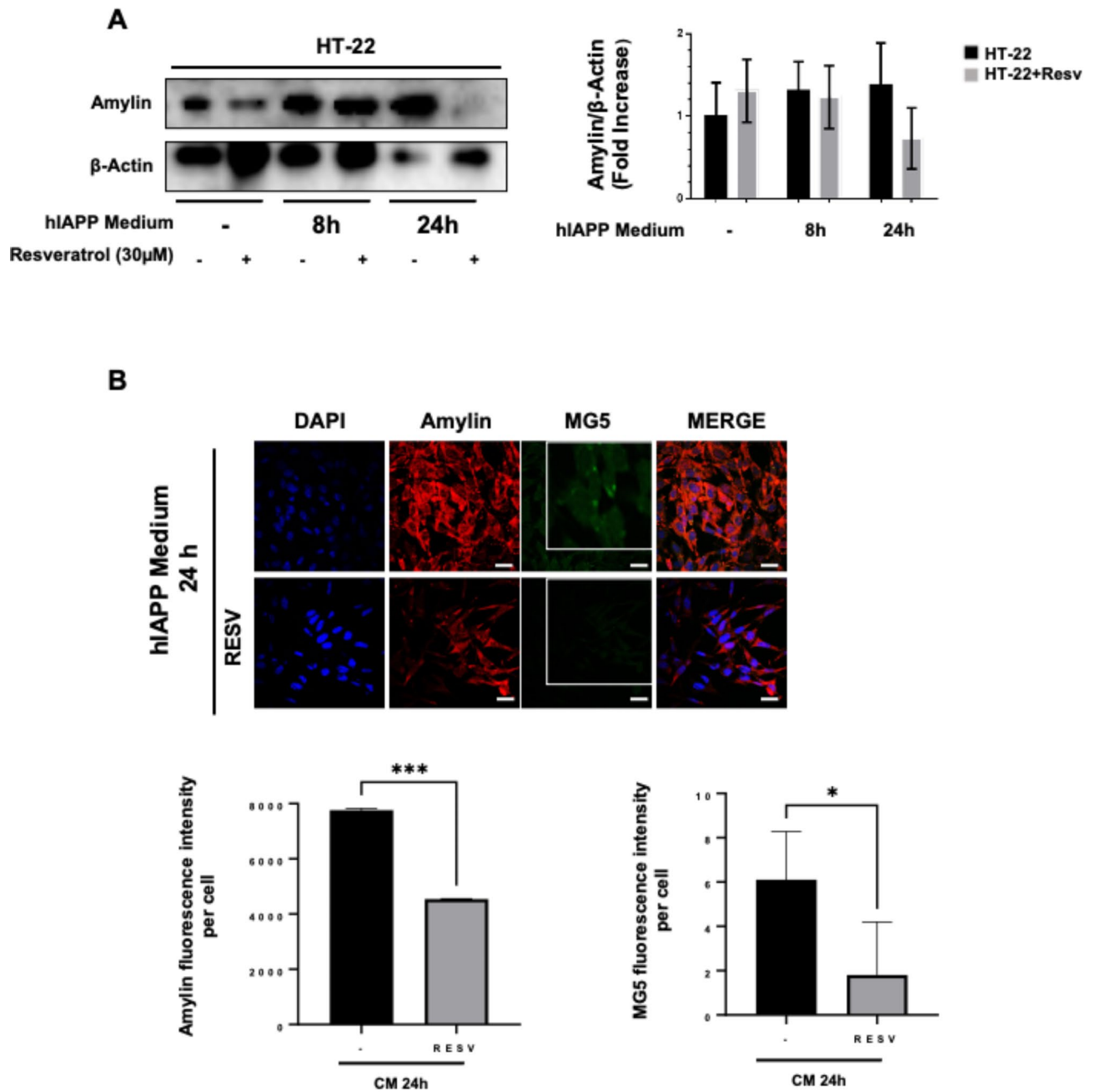


Fig. 5. Hippocampal cells HT-22 are protected from the aggregate-prone hIAPP medium with resveratrol. **(A)** Immunoblot analysis of amylin, using β actin as loading control, in the HT-22 cell lines exposed to conditioned media for 0, 8 and 24 h with and without Resveratrol 30 μ M 4 h ($n=5$). The plot indicates the quantification data of Amylin/ β -actin ratio under the different conditions. Data represent the mean \pm standard error of the mean (SEM) ($n=5$). **(B)** Immunofluorescence staining using an antibody against amylin and MG5 compound in the HT-22 cells exposed to conditioned media for 24 h with and without Resveratrol 30 μ M 4 h. DAPI staining was used to detect nuclei. The plot indicates the quantification data of both, amylin fluorescence intensity and MG5 fluorescence intensity under the different conditions. $**p < 0.01$; $***p < 0.0005$ by unpaired Student's *t*-test.

analysis. The accumulation of amylin and, notably, aggregates, diminished in the presence of resveratrol, thereby alleviating the stress in these cells at the 24-hour mark (Fig. 5B).

It's worth noting that, in contrast to what was observed in INS1E-hIAPP, no discernible changes in mitochondrial dynamics were detected in HT-22 cells (Supplementary Fig. 3).

Resveratrol protects HT-22 cells from the CM-induced mTORC1 activation and ER-stress

Subsequently, we chose to investigate the effects of CM on the recipient cells, specifically HT-22 cells. Notably, we observed a time-dependent reduction in the mTORC1 signaling pathway in response to resveratrol (Fig. 6A). Similarly, CM-induced endoplasmic reticulum (ER) stress exhibited a time-dependent increase, which was partially reversed upon treatment with resveratrol (Fig. 6B). Taken together, these findings suggest that resveratrol effectively mitigates the stress induced in HT-22 cells in response to conditioned media from INS1E-hIAPP.

Discussion

Amylin is a toxic protein and its overexpression in pancreatic β cells affect insulin secretion and the integrity of different membrane in different organelles, including cell membrane^{30,31}. In addition, we have observed that hIAPP can alter mitochondrial dynamics, autophagy and ER stress in INS1E-hIAPP cells⁹. But amylin can be transported to other regions and exert its deleterious effects in other cells. In this regard, we have published that amylin can be incorporated into EVs, modulating cell survival in the recipient cells²⁶. Here, we have determined that monomeric and soluble amylin expression can be modulated by treating the cells with resveratrol under both normal and high glucose conditions. When we determined amylin levels in INS1E-hIAPP cells under basal glucose conditions with resveratrol, we observed an important reduction in the total amount of amylin protein, by western blot analysis. Taking into account that, under basal glucose, there are low levels of amylin secretion, resveratrol could disrupt amylin aggregates³², generating more soluble amylin. Globally, these data suggest that resveratrol could facilitate amylin degradation, very likely by the induction of autophagy. In contrast, using immunofluorescence, there was an increase in soluble amylin, probably as consequence of the disaggregating capacity of resveratrol as it has previously mentioned. Under high glucose conditions, pancreatic β cells increase its secretion, although in this cell line, which overexpresses hIAPP, has been described an impairment in amylin and insulin secretion³⁰. In addition, under high glucose, there is an increased synthesis of soluble amylin, which could contribute for the production of new aggregates, because of the special conditions that occurs in INS1E-hIAPP cells, that contributes to the generation of misfolded hIAPP⁹. And, at the same time, there is an increased secretion of amylin in the interior of EVs (Fig. 4), contributing to the decrease in soluble amylin inside beta cells. Then, in western blot there is a net detection of the global amylin protein levels. In contrast, in immunofluorescence, there is a marked reduction in the soluble form of amylin. This net reduction in the soluble form of amylin, corresponds to different effects including, EVs-mediated amylin secretion, new aggregates that can be formed from the soluble amylin and the soluble amylin which has not been eliminated by the normal secretion. Then, it is plausible to suggest that, if in the western blot there is a global increase in amylin detection and in the immunofluorescence, there is huge reduction in amylin (in its soluble form), this increased in amylin detected in western blot is derived from the formation of new aggregates inside the cell. Importantly, when we added resveratrol under high glucose conditions, there was a net increase in the soluble form by immunofluorescence, which reflects the huge capacity of resveratrol in the disruption of aggregates in association with the inhibition of the incorporation of soluble amylin into the EVs. This is important because, the use of resveratrol can protect other cells from the deleterious effects of human amylin by different strategies including; (1) direct disaggregation capacity of resveratrol; (2) elimination through autophagy; 3 reducing the transport to other locations by EVs. These data indicate that resveratrol potentiates the solubility of the remaining amylin aggregates in the cell. In this regard, it has been proposed that resveratrol can interfere with the aggregation capacity of hIAPP^{33–36}. We interpret these paradoxical findings using these two techniques because in western blot we sonicated the samples and we probably disrupted amylin aggregates, favouring an increase in the total amount of amylin, as it has been previously described³⁷. In contrast, using immunofluorescence, we detected only soluble amylin and not the signal from the aggregates, demonstrating that both signals corresponding to amylin and MG5 compound do not colocalize using immunofluorescence in INS1E-hIAPP cells²⁶.

As it was described previously, mitochondrial dynamics represent mitochondria as a more dynamic organelle. Both processes, mitochondrial fusion and fission, are regulated by different factors including energy requirements^{24,25}. We have observed that in INS1E-WT cells in response to high glucose there is a switch towards mitochondrial fission. These changes are coherent with a situation of an increase in energy supply, which is counteracted with an increase in mitochondrial fragmentation for producing a decreased coupling of mitochondria and producing less energy²⁴. In contrast, in INS1E-hIAPP in response to high glucose there was maintenance in the mitochondrial fusion under normal glucose conditions. This situation of exaggerated fusion or fission is known as mitochondrial dysfunction and it is associated with T2DM³⁸. The increase in mTORC1 signalling pathway in INS1E-WT cells in response to resveratrol either under normal glucose or high glucose could be related with the increased production of amylin observed in these cells using immunofluorescence. This is coherent with previous data indicating that mTORC1 activity is involved in the control of secretion in pancreatic β cells³⁹. The observation indicating that in INS1E-hIAPP there was an increase in ER-stress in response to resveratrol, could be interpreted as a consequence of the stimulation of a canonical secretory capacity in these cells. However, when we added HG, we observed a reduction in ER-stress, and not modulated by resveratrol treatment. A possible explanation for these results is the induction of an alternative and non-canonical capacity of the cells under this situation, that could alleviate ER-stress. In this regard, under HG conditions we have determined a production of EVs, which includes amylin in the interior, representing an alternative pathway to eliminate the toxic protein. Although we have observed an increased production of EVs under mTORC1 overactivation in INS1E-hIAPP cells²⁶, just the opposite result has been obtained using MEF TSC2-/- cells⁴⁰. These results could be explained because the hyperactivation of mTORC1 that occurs in both cell lines is not the same and probably, it is necessary a certain threshold of mTORC1 hyperactivity to impair exosome release. Although resveratrol is a stilbene belonging to the polyphenols family, there is multiple evidence indicating its involvement in the mitochondrial quality control in different biological systems and the association with

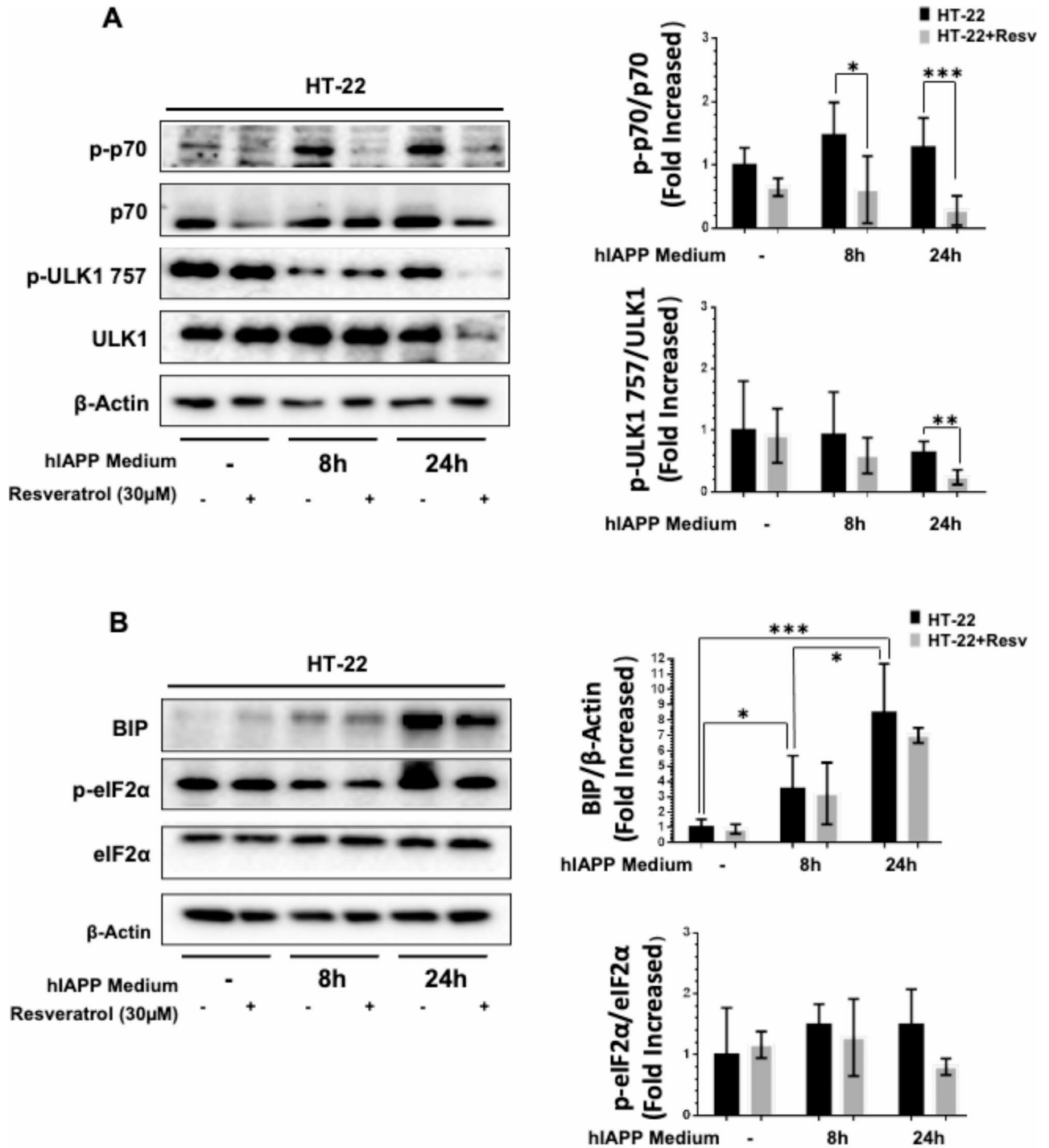


Figure 6

Fig. 6. Resveratrol protects HT-22 cells from the CM-induced mTORC1 activation and ER-stress. **(A)** Immunoblot analysis of p-p70, p70, p-ULK1 757, ULK1 using β actin as loading control, in the cell extracts of HT-22 cell lines exposed to conditioned media for 0, 8 and 24 h with and without Resveratrol 30 μ M 4 h ($n = 5$). The plot indicates the quantification data of Mfn1, Mfn2, p-p70/p70, p-ULK1 757/ULK1 ratio under the different conditions. Data represent the mean \pm standard error of the mean (SEM). * $p < 0.05$; ** $p < 0.01$; *** $p < 0.005$ by the use of unpaired Student's t -test. **(B)** Immunoblot analysis of BIP, p-eIF2 α , eIF2 α , p-PERK, PERK, using β actin as loading control, in the cell extracts of HT-22 cell lines exposed to conditioned media for 0, 8 and 24 h with and without Resveratrol 30 μ M 4 h ($n = 5$) The plot indicates the quantification data of BIP, p-eIF2 α /eIF2 α , p-PERK/PERK ratio under the different conditions. Data represent the mean \pm standard error of the mean (SEM). * $p < 0.05$; *** $p < 0.005$ by unpaired Student's t -test.

different diseases^{41–44}. The association between T2DM and neurodegeneration is evident as it is indicated in the literature^{13,14,45–47}. Specifically, amylin has been proposed as one of the possible molecular links between T2DM and Alzheimer's disease^{15,17,48}. Using the HT-22 cell line as an in vitro model of hippocampal cells, we uncovered that at basal conditions we were able to detect amylin protein. This was an unexpected result but, it is described that amylin can be produced in different brain areas, including the dentate gyrus of the hippocampus⁴⁹. When we exposed HT-22 to the CM obtained from INS1E-hIAPP we observed an accumulation of amylin as well as an increase in aggregates in a time-dependent manner. The aggregation capacity of the CM was totally blunted when we used an inhibitor of endocytosis, indicating that amylin is incorporated using this mechanism. This is important since, these data suggest that the toxic effects of amylin observed in HT-22 hippocampal cells is not mediated by soluble amylin using an amylin-receptor dependent mechanism, and probably by alternative mechanisms such as extracellular vesicles or exosomes. In this regard, in the EVs isolated from INS1E-hIAPP we were able to detect amylin in its interior, as we previously demonstrated²⁶. Very interestingly, previous reports indicate that using different concentrations of amylin, for the induction of oligomeric forms of amylin, could be integrated in pancreatic β cells through an endocytosis-dependent mechanism. However, the authors indicate that the use of endocytic inhibitors were effective in preventing the internalization of soluble amylin oligomers⁵⁰. The idea of the transport of toxic proteins and the spread of the disease to other locations using alternative mechanisms, is not new and it has been described in both Alzheimer's disease and Parkinson's disease^{51,52}. The aggregates observed in HT-22 after the exposition to the CM obtained from INS1E-hIAPP was greatly reduced after the addition of resveratrol. These effects have been examined before with these compounds and other synthetic derivatives, being implicated in the inhibition of aggregation of amyloid proteins in both Alzheimer's and Parkinson's disease^{53,54}. Resveratrol treatment in HT-22 cells decreased the mTORC1 signalling pathway induced by the CM obtained from INS1E-hIAPP. These data indicate that resveratrol could induce autophagy for the elimination of aggregates and reducing the associated ER-stress. Similar results have been obtained in other organisms in which resveratrol protects from Alzheimer's disease, diminishing the A β -induced toxicity in a *C. elegans* model⁵⁵. Very importantly, resveratrol treatment in INS1E-hIAPP cells decreased the EV size, with the generation of two additional peaks of EVs with a smaller size in the DLS analysis. These data indicate that resveratrol could impair the formation of bigger EVs, obtained under HG conditions, which suggest a direct link between EVs size and the aggregation capacity of hIAPP. In fact, a similar effect has been described using the neuroblastoma cell line SHSY5Y, proposing that resveratrol disrupts A β 1–42 aggregation by the induction of A β 1–42 fragmentation into smaller peptides, with a very low propensity to aggregate⁵⁴.

Conclusion

In summary, we have uncovered that resveratrol is a potent inhibitor of the aggregation capacity of amylin found in INS1E-hIAPP and it is able to diminish the deleterious effects, as a consequence of the spreading of the toxic protein, to other cell types such as the hippocampal cells, HT-22. In Fig. 7, we depict the main findings found in this manuscript about the role of resveratrol in the control of the amylin aggregating-prone capacity in pancreatic β cells as well as in hippocampal cells.

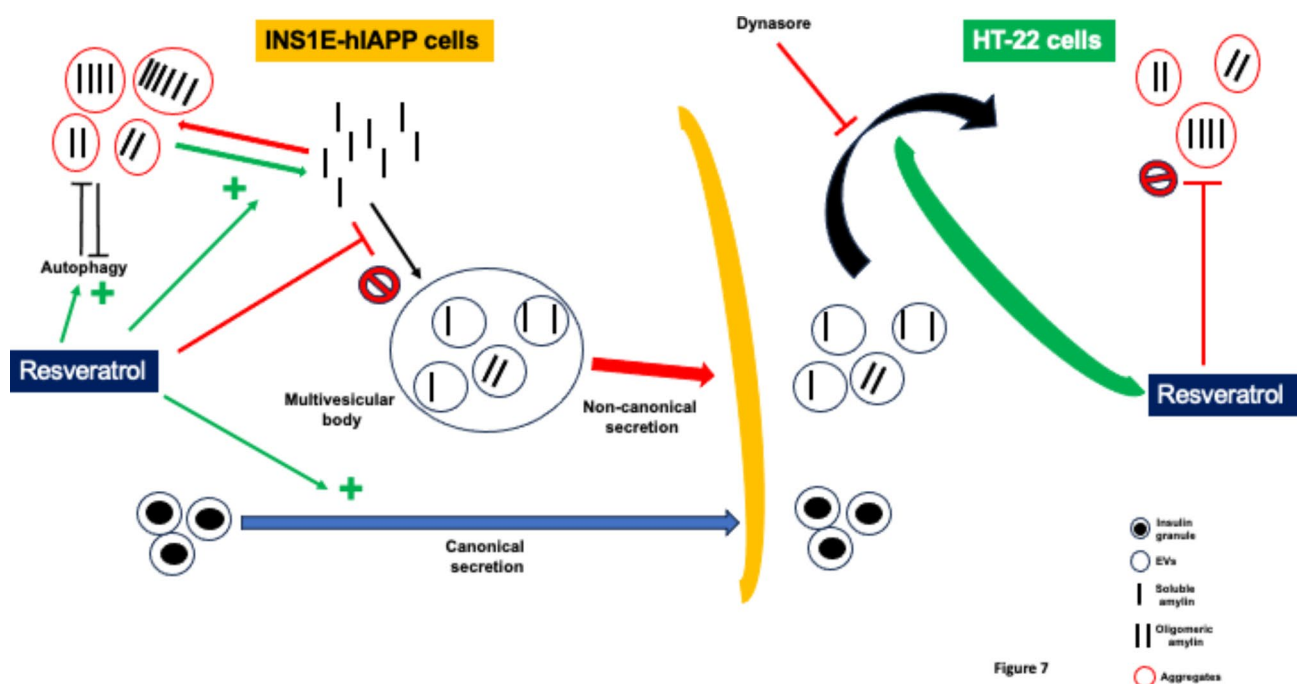


Fig. 7. Scheme depicting the most important findings related with the protective role of resveratrol in the control of the human amylin aggregating-prone capacity in pancreatic β cells as well as in hippocampal cells.

Data availability

All data supporting the findings of this study are available in the Supplementary Information.

Received: 9 July 2024; Accepted: 5 November 2024

Published online: 11 November 2024

References

- Saisho, Y. Changing the concept of type 2 diabetes: beta cell workload hypothesis revisited. *Endocr. Metab. Immune Disord. Drug Targets*. **19**, 121–127 (2019).
- Guillén, C. & Benito, M. mTORC1 overactivation as a key aging factor in the progression to type 2 diabetes Mellitus. *Front. Endocrinol. (Lausanne)* **9**, 621 (2018).
- You, S., Zheng, J., Chen, Y. & Huang, H. Research progress on the mechanism of beta-cell apoptosis in type 2 diabetes mellitus. *Front. Endocrinol. (Lausanne)* **13**, 976465 (2022).
- Benáková, S., Holendová, B. & Plecítá-Hlavatá, L. Redox homeostasis in pancreatic β -Cells: from development to failure. *Antioxidants (Basel)* **10**, 526 (2021).
- Talchai, C., Xuan, S., Lin, H. V., Sussel, L. & Accili, D. Pancreatic β cell dedifferentiation as a mechanism of diabetic β cell failure. *Cell*. **150**, 1223–1234. <https://doi.org/10.1016/j.cell.2012.07.029> (2012).
- Kiriyama, Y. & Nochi, H. Role and cytotoxicity of amylin and protection of pancreatic islet β -cells from amylin cytotoxicity. *Cells* **7**, 95 (2018).
- Westermarck, P., Andersson, A. & Westermarck, G. T. Islet amyloid polypeptide, islet amyloid, and diabetes mellitus. *Physiol. Rev.* **91**, 795–826 (2011).
- Akter, R. et al. Islet amyloid polypeptide: structure, function, and pathophysiology. *J. Diabetes Res.* **2016**, 2798269. (2016).
- García-Hernández, M. et al. Pancreatic β cells overexpressing hIAPP impaired mitophagy and unbalanced mitochondrial dynamics. *Cell. Death Dis.* **9**, 481 (2018).
- Szwd, A., Kim, E. & Jacinto, E. Regulation and metabolic functions of mTORC1 and mTORC2. *Physiol. Rev.* **101**, 1371–1426 (2021).
- Appenzeller-Herzog, C. & Hall, M. N. Bidirectional crosstalk between endoplasmic reticulum stress and mTOR signaling. *Trends Cell Biol.* **22**, 274–282 (2012).
- Hetz, C., Zhang, K. & Kaufman, R. J. Mechanisms, regulation and functions of the unfolded protein response. *Nat. Rev. Mol. Cell Biol.* **21**, 421–438 (2020).
- Madhusudhanan, J., Suresh, G. & Devanathan, V. Neurodegeneration in type 2 diabetes: Alzheimer's as a case study. *Brain Behav.* **10**, e01577 (2020).
- Burillo, J. et al. Insulin resistance and diabetes mellitus in Alzheimer's disease. *Cells* **10**, 1236 (2021).
- Martínez-Valbuena, I. et al. Amylin as a potential link between type 2 diabetes and Alzheimer disease. *Ann. Neurol.* **86**, 539–551 (2019).
- Bharadwaj, P. et al. The link between type 2 diabetes and neurodegeneration: roles for Amyloid- β , Amylin, and Tau Proteins. *J. Alzheimers Dis.* **59**, 421–432 (2017).
- Wijesekara, N. et al. Amyloid- β and islet amyloid pathologies link Alzheimer's disease and type 2 diabetes in a transgenic model. *FASEB J.* **31**, 5409–5418 (2017).
- Ho, G. et al. Connecting Alzheimer's disease with diabetes mellitus through amyloidogenic evolvability. *Front. Aging Neurosci.* **12**, 576192 (2020).
- Guerrero-Muñoz, M. J., Castillo-Carranza, D. L. & Kaye, R. Therapeutic approaches against common structural features of toxic oligomers shared by multiple amyloidogenic proteins. *Biochem. Pharmacol.* **88**, 468–478 (2014).
- Fantacuzzi, M., Amoroso, R., Carradori, S. & De Filippis, B. Resveratrol-based compounds and neurodegeneration: recent insight in multitarget therapy. *Eur. J. Med. Chem.*, 233114242. (2022).
- Marambaud, P., Zhao, H. & Davies, P. Resveratrol promotes clearance of Alzheimer's disease amyloid- β peptides. *J. Biol. Chem.* **280**, 37377–37382 (2005).
- Freyssin, A., Page, G., Fauconneau, B. & Bilan, A. R. Natural stilbenes effects in animal models of Alzheimer's disease. *Neural Regen. Res.* **15**, 843–849 (2020).
- Paul, S., Saha, D. & Bk, B. Mitochondrial dysfunction and mitophagy closely cooperate in neurological deficits associated with alzheimer's disease and type 2 diabetes. *Mol. Neurobiol.* **58**, 3677–3691 (2021).
- Liesa, M. & Shirihai, O. S. Mitochondrial dynamics in the regulation of nutrient utilization and energy expenditure. *Cell. Metab.* **17**, 491–506 (2013).
- Chan, D. C. Mitochondrial dynamics and its involvement in disease. *Annu. Rev. Pathol.* **15**, 235–259 (2020).
- Burillo, J. et al. Human amylin aggregates release within exosomes as a protective mechanism in pancreatic β cells: pancreatic β -hippocampal cell communication. *Biochim. Biophys. Acta Mol. Cell. Res.* **1868**, 118971 (2021).
- Tu, L.-H. et al. Mutational analysis of the ability of resveratrol to inhibit amyloid formation by islet amyloid polypeptide: critical evaluation of the importance of aromatic-inhibitor and histidine-inhibitor interactions. *Biochemistry* **54**, 666–676 (2015).
- Lolicato, F., Raudino, A., Milardi, D. & La Rosa, C. Resveratrol interferes with the aggregation of membrane-bound human-IAPP: a molecular dynamics study. *Eur. J. Med. Chem.* **92**, 876–881 (2015).
- Jiang, P., Li, W., Shea, J.-E. & Mu, Y. Resveratrol inhibits the formation of multiple-layered β -sheet oligomers of the human islet amyloid polypeptide segment 22–27. *Biophys. J.* **100**, 1550–1558 (2011).
- Pithadia, A., Brender, J. R., Fierke, C. A. & Ramamoorthy, A. Inhibition of IAPP aggregation and toxicity by natural products and derivatives. *J. Diabetes Res.* **2016**, 2046327 (2016).
- Sciacca, M. F. M. et al. A blend of two resveratrol derivatives abolishes hIAPP amyloid growth and membrane damage. *Biochim. Biophys. Acta Biomembr.* **1860**, 1793–1802 (2018).
- Chatani, E. et al. Ultrasonication-dependent production and breakdown lead to minimum-sized amyloid fibrils. *Proc. Natl. Acad. Sci. USA.* **106**, 1119–1124 (2009).
- Díaz-Vegas, A. et al. Is mitochondrial dysfunction a common root of noncommunicable chronic diseases? *Endocr. Rev.* **41**, 1–27 (2020).

39. Israeli, T. et al. Nutrient Sensor mTORC1 regulates insulin secretion by modulating β -cell autophagy. *Diabetes* **71**, 453–469 (2022).
40. Zou, W. et al. Exosome release is regulated by mTORC1. *Adv. Sci. (Weinh)* **6**, 1801313 (2018).
41. Kung, H.-C., Lin, K.-J., Kung, C.-T. & Lin, T.-K. Oxidative stress, mitochondrial dysfunction, and neuroprotection of polyphenols with respect to resveratrol in Parkinson's disease. *Biomedicines* **9**, 918 (2021).
42. Wang, N. et al. Exploration of age-related mitochondria dysfunction and the anti-aging effects of resveratrol in zebrafish retina. *Aging (Albany NY)* **11**, 3117–3137 (2019).
43. Wang, D. et al. Resveratrol improves muscle atrophy by modulating mitochondrial quality control in STZ-induced diabetic mice. *Mol. Nutr. Food Res.* **62**, e1700941 (2018).
44. Ren, X. et al. Resveratrol ameliorates mitochondrial elongation via Drp1/Parkin/PINK1 signaling in senescent-like cardiomyocytes. *Oxid. Med. Cell Longev.* **2017**, 4175353 (2017).
45. Cheong, J. L. Y., De Pablo-Fernández, E., Foltyniec, T. & Noyce, A. J. The association between type 2 diabetes mellitus and Parkinson's disease. *J. Parkinsons Dis.* **10**, 775–789 (2020).
46. Lynn, J., Park, M., Ogunwale, C. & Acquah-Mensah, G. A tale of two diseases: exploring mechanisms linking diabetes mellitus with Alzheimer's disease. *J. Alzheimers Dis.* **85**, 485–501 (2022).
47. Biosa, A., Outeiro, T. F., Bubacco, L. & Bisaglia, M. Diabetes mellitus as a risk factor for Parkinson's disease: a molecular point of view. *Mol. Neurobiol.* **55**, 8754–8763 (2018).
48. Raimundo, A. F., Ferreira, S., Martins, I. C. & Menezes, R. Islet amyloid polypeptide: a partner in crime with A β in the pathology of Alzheimer's disease. *Front. Mol. Neurosci.* **13**, 35 (2020).
49. Yoo, Y.-M., Jung, E.-M., Jeung, E.-B., Jo, B. R. & Joo, S. S. Amylin protein expression in the rat brain and Neuro-2a cells. *Int. J. Mol. Sci.* **23**, 4348 (2022).
50. Trikha, S. & Jeremic, A. M. Clustering and internalization of toxic amylin oligomers in pancreatic cells require plasma membrane cholesterol. *J. Biol. Chem.* **286**, 36086–36097 (2011).
51. Stundl, A. et al. α -synuclein in plasma-derived extracellular vesicles is a potential biomarker of Parkinson's disease. *Mov. Disord.* **36**, 2508–2518 (2021).
52. Gomes, P. et al. Extracellular vesicles and Alzheimer's disease I the novel era of precision medicine: implications for disease progression, diagnosis and treatment. *Exp. Neurol.* **358**, 114183 (2022).
53. Chau, E., Kim, H., Shin, J., Martínez, A. & Kim, J. R. Inhibition of alpha-synuclein aggregation by AM17, a synthetic resveratrol derivative. *Biochem. Biophys. Res. Commun.* **574**, 85–90 (2021).
54. Al-Edresi, S., Alsalahat, I., Freeman, S., Aojula, H. & Penny, J. Resveratrol-mediated cleavage of amyloid β_{1-42} peptide: potential relevance to Alzheimer's disease. *Neurobiol. Aging* **94**, 24–33 (2020).
55. Regitz, C., Fitzenberger, E., Mahn, F. L., Dußling, L. M. & Wenzel, U. Resveratrol reduces amyloid-beta (A β_{1-42})-induced paralysis through targeting proteostasis in an Alzheimer model of *Caenorhabditis elegans*. *Eur. J. Nutr.* **55**, 741–747 (2016).

Acknowledgements

We thank Programa Investigo for funding Carlos González-Blanco, and Elena González for her assistance in the laboratory. We thank the immunofluorescence facility core from the Complutense University of Madrid for their technical assistance. We thank to P2022/BMD-7227, MOIR-ACTOME-CM. Dirección General de Investigación e Innovación Tecnológica (DGIIT). Consejería de Educación y Universidades. Comunidad de Madrid. Madrid, España. Rat insulinoma cell line INS1E-WT cells were kindly provided by P. Maechler (Université de Genève, Geneva, Switzerland); INS1E overexpressing human amylin (INS1E-hIAPP) were generously supplied by Anna Novials (IDIBAPS, Barcelona, Spain). Mouse hippocampal cell line HT-22 was gently donated by Rafael Simó (Vall D'Hebron Research Institute, Barcelona, Spain). We thank to José Carlos Menéndez from the Department of Organic Chemistry for generously giving us MG5 and Thioflavin T compounds for the detection of amylin aggregates.

Author contributions

Author Contributions: The individual role of all the authors in the present manuscript are the following: Conceptualization, C.G.; methodology, C. G.-B., A.C.L.; software, C.G.; validation, C.G., C.G.-B.; formal analysis, C.G., C. G.-B.; investigation, C. G.-B., A.C.L.; resources, G.G.; data curation, C.G.; writing—original draft preparation, C.G., C. G.-B.; writing—review and editing, C. G.-B., A.C.L., S.I-F, B.J., P.M., C.F., A. G-A, M.B., C.G.; visualization, C. G.-B., C.G.; supervision, C.G., G.G.; project administration, C.G., M.B. All authors have read and agreed to the published version of the manuscript.

Funding

This work was supported by grants PID2020-113361RB-I00 from Ministerio de Ciencia e Innovación and CIBER de Diabetes y Enfermedades Metabólicas Asociadas, Instituto de Salud Carlos III (Spain), to C. Guillén and M. Benito.

Declarations

Competing interests

The authors declare no competing interests.

Additional information

Supplementary Information The online version contains supplementary material available at <https://doi.org/10.1038/s41598-024-78967-2>.

Correspondence and requests for materials should be addressed to C.G.

Reprints and permissions information is available at www.nature.com/reprints.

Publisher's note Springer Nature remains neutral with regard to jurisdictional claims in published maps and institutional affiliations.

Open Access This article is licensed under a Creative Commons Attribution-NonCommercial-NoDerivatives 4.0 International License, which permits any non-commercial use, sharing, distribution and reproduction in any medium or format, as long as you give appropriate credit to the original author(s) and the source, provide a link to the Creative Commons licence, and indicate if you modified the licensed material. You do not have permission under this licence to share adapted material derived from this article or parts of it. The images or other third party material in this article are included in the article's Creative Commons licence, unless indicated otherwise in a credit line to the material. If material is not included in the article's Creative Commons licence and your intended use is not permitted by statutory regulation or exceeds the permitted use, you will need to obtain permission directly from the copyright holder. To view a copy of this licence, visit <http://creativecommons.org/licenses/by-nc-nd/4.0/>.

© The Author(s) 2024